A&A, 707, A326 (2026)
https://doi.org/10.1051/0004-6361/202557753

Astronomy & Astrophysics

The hybrid Nova Vul 2024 (=V615 Vul)

P. Valisa[1,⋆], U. Munari[2], and I. Albanese[3]

[1] ANS Collaboration, c/o Astronomical Observatory, 36012 Asiago (VI), Italy
[2] INAF National Institute of Astrophysics, Astronomical Observatory of Padova, 36012 Asiago (VI), Italy
[3] Dept. of Physics and Astronomy, University of Padova, Asiago Astrophysical Observatory, 36012 Asiago (VI), Italy

Received 19 October 2025 / Accepted 16 February 2026

ABSTRACT

Context. Among galactic novae, many remain poorly characterized due to heterogeneous data, observational challenges, or heavy reddening along the Galactic plane. A detailed characterization is particularly crucial for novae exhibiting peculiar features, such as those belonging to the hybrid class.
Aims. We present the spectroscopic and photometric evolution of the heavily reddened Nova Vul 2024 (=V615 Vul) from discovery on 29 July 2024 to well into its nebular phase.
Methods. We obtained daily optical, absolute-fluxed spectroscopy in both low- and high-resolution echelle modes, providing a detailed account of the spectral evolution. Photometric data were primarily sourced from AAVSO, while refined astrometry was performed to assess the positional coincidence with a potential progenitor. Robust determinations of t_3 and E_{B-V} were achieved, allowing for the application of the Maximum Magnitude–Rate of Decline (MMRD) relation; the resulting distance is in excellent agreement with 3D Galactic extinction maps.
Results. Nova Vul 2024 is a very fast nova ($t_3 = 10.7 \pm 0.5$ d) located at a distance of 5.0 ± 1.0 kpc, suffering from a large reddening ($E_{B-V} = 1.6 \pm 0.1$). Around maximum light, it exhibited a Fe II-type spectrum with very broad emission lines (FWZI $\approx 5800\,\mathrm{km\,s^{-1}}$) and high-velocity P-Cygni absorptions. Following t_3, coinciding with the emergence of hard X-ray emission, the nova displayed pronounced photometric oscillations primarily driven by continuum variations. Simultaneously, He/N features developed alongside Fe II lines, classifying V615 Vul as a rare hybrid nova. During the nebular phase, the ionization level increased, reaching [Fe VII] and likely [Fe X]. The ejecta showed no neon overabundance and expanded ballistically, as indicated by the constant widths, profiles, and castellation of the high-resolution emission lines.

Key words. novae, cataclysmic variables

1. Introduction

Classical novae are powered by a sudden thermonuclear runaway of hydrogen-rich material that is accreted onto the surface of a white dwarf from a low-mass companion in a close binary system (Warner 1995). The outburst results in a dramatic increase in luminosity and the ejection of non-equilibrium CNO-burning products at velocities ranging from a few hundred to a few thousand km/s. Based on early-time ejecta spectra, novae are classified by Williams (1992) into two main spectroscopic classes: those characterized by prominent Fe II emission lines and those dominated by He/N emission lines. A small fraction of novae exhibit hybrid behaviour, evolving from the Fe II to the He/N class.

Nova Vul 2024 (=PNV J19430751+2100204 = V615 Vul; NVul24 for short) was discovered on 2024 July 29.832 UT, just a few hours before passing through photometric maximum, in wide field unfiltered images obtained by Sokolovsky et al. (2024c) with a 135 mm f/2.0 telephoto lens in the framework of the New Milky Way Survey operating at the Astroverty astrofarm in Nizhnii Arkhyz, Karachay-Cherkessia, Russia.

The object was classified soon thereafter as a reddened classical nova by Taguchi (2024) based on an optical spectrum obtained on July 30.47 UT. Compared to Taguchi's spectrum, all emission lines appeared weaker in an echelle spectrum recorded by Valisa & Munari (2024) nine hours later on 30.87 UT, a decline typical of novae quickly rising towards maximum brightness. On Jul 30.87 UT the Swift satellite pointed to the nova, but no X-ray emission was detected (Sokolovsky et al. 2024b). Detection of hard X-rays from shock-heated plasma within the nova ejecta finally came around day +11 and persisted through to day +24 (Sokolovsky et al. 2024a).

In this paper we present a detailed analysis of NVul24 based on the photometric evolution as recorded by the American Association of Variable Star Observers (AAVSO) and the Zwicky Transient Facility (ZTF) (Masci et al. 2019) and on our intensive spectroscopic monitoring that collected 31 spectra of the nova, on a daily basis during the first 20 days following its discovery, and then at a reduced cadence up to day +118, well into the advanced nebular phase. Particular attention is given to the transition from the initial FeII-type to a He/N-type spectrum on day +11, which identifies NVul24 as a new member of the elusive class of hybrid novae. The emergence of the He/N spectrum occurred simultaneously with the onset of photometric oscillations and with the transformation of the Hα profile from that typical of optically thick conditions to that characteristic of an optically thin shell.

2. Observations

2.1. Spectroscopy

Spectra of NVul24 were recorded both at high resolution and at low dispersion with long-slit spectrographs. A logbook of the spectroscopic observations is provided in Appendix A. We collected a total of 31 spectra distributed over 28 individual nights

⋆ Corresponding author: paolo.valisa@astrogeo.va.it

spanning the period from discovery to day +118 after the outburst, when NVul24 had already faded seven magnitudes from maximum and was well into the nebular phase.

Most of the high-resolution (Echelle) spectra have been obtained with the Varese Schiaparelli Observatory 0.84 m telescope, which is operated by ANS Collaboration. The telescope is equipped with an Astrolight Inst. mk.III Multi-Mode carbon-fibre spectrograph, which in the Echelle configuration covers the 4250–8900 Å range (cf. Munari & Valisa 2014, for an optical description and performance evaluation of these multi-mode spectrographs). Cross-dispersion is achieved with a N-SF11 prism, and the detector is an SBIG ST10XME CCD camera (2192 × 1472 array, 6.8 µm pixel, KAF-3200ME chip with micro-lenses to boost the quantum efficiency). The spectral resolution obtained with a R2 79 l/mm grating is 20 000 for a 1-arcsec slit and CCD binning = 1×, lowering to 15 000 for a 2-arcsec slit, and 12 000 for CCD binning = 2×. Only the two reddest orders are affected by inter-order gaps, between 8239–8243 Å and 8554–8574 Å.

One additional Echelle spectrum, at a later epoch when NVul24 became fainter than $R = 13$, was collected using the 1.82 m telescope + REOSC Echelle spectrograph which is operated in Asiago by INAF (Italian National Institute of Astrophysics). The 3500–7350 Å interval is covered over 32 orders without inter-order gaps by an Andor DW436-BV camera (housing a 2048 × 2048 array, 13.5 µm pixel size, E2V CCD42-40 AIMO model CCD). The resolving power is 22 000 for the standard 1.8-arcsec slit width.

Low-dispersion spectra were acquired with the B&C spectrograph on the 1.22 m telescope operated in Asiago by the University of Padova. The spectra were obtained with a 300 ln/mm grating blazed at 5000 Å, which covers the 3200–8000 Å range at 2.3 Å/pix dispersion. The detector was a 2048 × 512 ANDOR iDus DU440A E2V 42-10 back-illuminated CCD. This setup offers excellent sensitivity in the near-UV down to 3200 Å.

All observations at all telescopes were conducted with the slit oriented along the parallactic angle, for optimal sky-subtraction and flux calibration. Data reduction for all telescopes has been performed in IRAF and has included all usual steps for bias, dark, flat, long-slit sky subtraction, wavelength calibration, heliocentric correction, and flux calibration. The absolute flux calibration was obtained via nightly observations of the spectrophotometric standard HR 7596, located on the sky close to the nova. This allowed us to join all Echelle orders into a single 1D-fluxed spectrum covering the whole recorded wavelength range. The flux zero point of each spectrum has been checked against the near-simultaneous *BVRI* data from AAVSO.

2.2. Photometry

BVRI photometric observations of NVul24 were retrieved from the American Association of Variable Star Observers (AAVSO) database. The high cadence of these data up to day +50 allowed for binning into 0.5-day intervals, effectively reducing the scatter. Within each bin, the average difference between the minimum and maximum V-band magnitude is 0.4 mag, with a standard error of the mean of approximately 0.1 mag. At later epochs, the lower sampling density increases the uncertainty per interval.

The discrepancies between measurements from different observers likely arise from a lack of transformation to the standard BVRI system. Furthermore, the intense Hα emission, which overlaps with the red wing of the V-band transmission profile, may significantly affect the photometry depending on the specific filter response of each observer. Finally, ZTF g- and r-band photometry was obtained through the ZTF Forced Photometry Service (Masci et al. 2019).

3. Photometric evolution

The AAVSO and ZTF light- and colour-curves of NVul24 covering the first 120 days of the outburst are presented in Fig. 1. The rise to maximum, the passage at peak brightness, and the early decline were rapid, smooth, and well-mapped by the observations. From the light curve in Fig. 1 we derive as the time of maximum in V band HJD = 2460522.3 (=2024 Jul. 30.8 UT), which we will adopt as the t_0 reference epoch in this paper.

The rise time to maximum brightness was less than 2 days, since the latest reported non-detection was 2024 Jul. 28.840 UT (at a limiting mag 14.5, cf. CBET 5423). The time required to decline by two and three magnitudes from maximum were $t_2 = 5 \pm 0.5$ and $t_3 = 10.7 \pm 0.5$ days, respectively, which are typical of very fast novae according to the classification scheme of Warner (1995). The small value of t_2 makes NVul24 one of the fastest FeII novae of recent years. Other very fast novae of the FeII class include N Cyg 2005 (V2361 Cyg, $t_2 = 6.0$ days; Hachisu & Kato 2007), N Aql 1999 (V1494 Aql, $t_2 = 6.6$ days; Kiss & Thomson 2000), N Cyg 2007 (V2467 Cyg, $t_2 = 7$ days; Schwarz et al. 2011), and N Cyg 2008 (V2468 Cyg, $t_2 = 7.8$ days; Iijima & Naito 2011). Recent novae faster than NVul 24 all belong to the He/N class, such as N Cyg 2001 N2 (V2275 Cyg, $t_2 = 2.9$ days; Kiss et al. 2002) and N Her 2021 (V1674 Her, $t_2 = 1$ days; Woodward et al. 2021).

Overall, the light curve of NVul24 resembles the 'O' class (oscillating novae) according to Strope et al. (2010), with an initially smooth decline and quasi-periodic oscillations of ≈1 magnitude amplitude, starting around the passage at t_3 and lasting to about day +70 (the increasing noise in the AAVSO data at later epochs makes it difficult to discern if oscillations were persisting after that epoch). The time-scale of the oscillations increased from an initial value of 5–6 days, to 9–12 days around day +70. Some other novae share this same photometric behaviour (of a lengthening with time of the oscillation time scale), including V603 Aql, V1494 Aql (Iijima & Naito 2011), V4745 Sgr (Csák et al. 2005), V888 Cen (Strope et al. 2010) and V2467 Cyg (Poggiani 2009).

In general, O-class light curves after the peak are well described by a broken power-law of the form $F^V_{\rm decline} \propto (t - t_0)^\alpha$ (Hachisu & Kato 2006; Strope et al. 2010). As shown in Fig. 2, NVul24 conforms to that with $\alpha = -1.48 \pm 0.05$ from t_2 to about day +75, and $\alpha = -2.2 \pm 0.1$ after that. The change in the slope of the broken power-law may relate to the end of the nuclear burning in the shell of the WD, implying a cooling of its surface temperature and consequently a decline in the feeding to the ejecta of high-energy photons able to contrast the ion recombination. Although information on the SSS phase in NVul24 is not available, evidence suggesting that the end of the SSS phase may influence the decay slope of several emission lines was reported by Azzollini et al. (2023) in a detailed study of RS Oph. Hachisu & Kato (2006) preferred a different interpretation, with the transition in the broken power-law marking the time at which stops the wind that they propose is continuously blowing-off the WD since early times in the outburst.

The colour evolution of NVul24 follows the average evolution observed in novae, as discussed by Craig et al. (2025). The $(B-V)$ evolution towards bluer colours reflects the shift at shorter wavelength of the maximum of the blackbody-like emission of

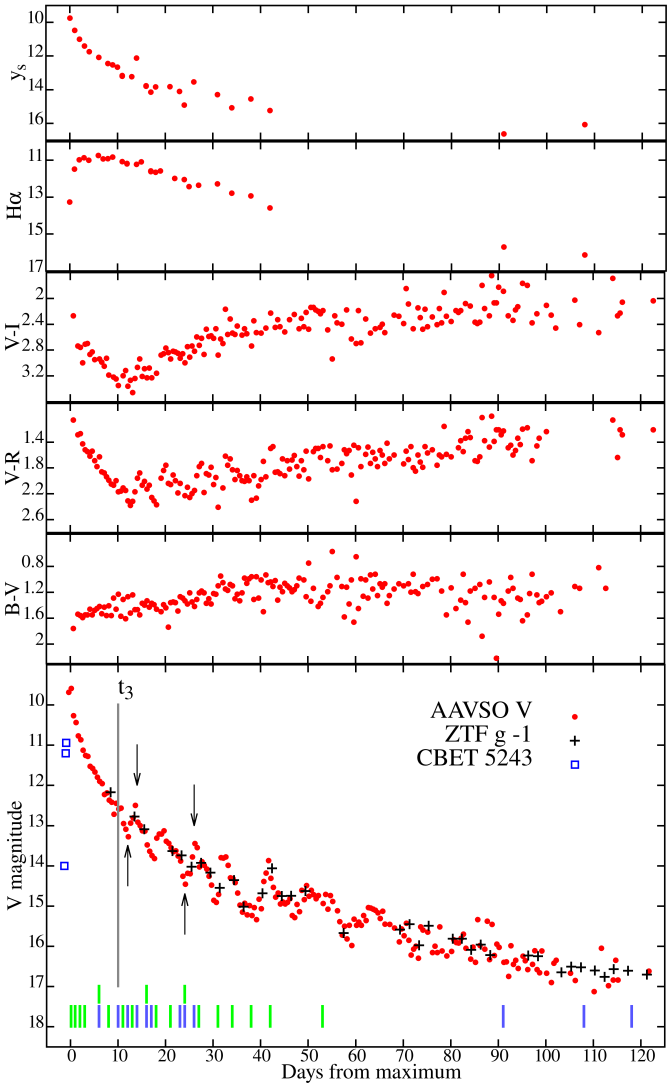

Fig. 1. Colour and light curves of Nova Vul 2024. The Strömgren y-band magnitude and the Hα emission-line flux, expressed in magnitudes, are obtained by integrating the flux-calibrated spectra. Black dots are ZTF g magnitudes rescaled to AAVSO V magnitudes by adding a -1 mag offset. The observing epochs are counted as days passed since optical maximum (2024 Jul. 30.8 UT). The green ticks in the V-band panel mark the epoch of Echelle observations, while the blue ticks are the epochs of low resolution spectra. The arrows point to epochs of spectra shown in Fig. 7 that were obtained at minima and maxima during oscillation period.

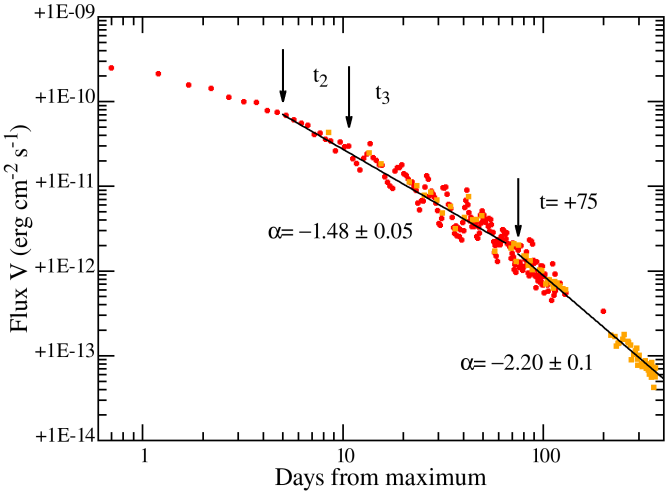

Fig. 2. Log-log plot of the time evolution of the flux radiated by NVul24 through the V band. The fit with a broken power-law of the form $F^V \propto (t - t_0)^\alpha$ is overplotted (lines in black) and the corresponding values of α are quoted. Red dots are from AAVSO magnitudes, binned each half-day. Orange dots are from ZTF g magnitudes rescaled to V magnitudes by adding a -1 mag offset.

the pseudo-photosphere while it retraces through the ejecta as their density decline because of the expansion. To separate the role of emission lines and underlying continuum in governing the behaviour of colours, on our accurately fluxed spectra we have measured separately the flux of the Hα emission line and that in the y Stromgren band (which is remarkably free for the presence of significant emission lines through the whole evolution of a normal nova (Hachisu et al. 2008) and plotted them at the top of Fig. 1. The flux zero-point for the R band has been adopted for Hα too. It is rather clear how the $(V - R)$ colour is dominated up to t_3 by the great contribution from Hα, similarly to $(V - I)$ colour by OI 8446 which is pumped by Lyman-β fluorescence. Past t_3, both Hα and OI 8446 accelerate their decline matching the pace of the underlying continuum, with the net result that both $(V - R)$ and $(V - I)$ became bluer with time for the same reasons as for $(B - V)$.

4. Reddening and distance estimates

An estimate of the reddening of NVul24 was obtained by Valisa & Munari (2024) from an echelle spectrum recorded on July 30.869 UT. A value $E_{B-V} = 1.7$ mag was derived from the equivalent width (EW) the diffuse interstellar band (DIB) at 6614 Å, using the calibration by Munari (2014), and a similar $E_{B-V} = 1.75$ mag was derived from the EW of interstellar KI 7699 Å line, following the calibration of Munari & Zwitter (1997).

A high reddening affecting NVul24 is confirmed by other indicators. For the DIBs at 5780 and 5797 Å we measure an EW of 0.78 and 0.34 Å, respectively, implying $E_{B-V} = 1.6$ for both of them from the calibrations of Kos & Zwitter (2013). van den Bergh & Younger (1987) reported the intrinsic colour of novae as $(B-V)_\circ = +0.23$ and -0.02 when passing at maximum brightness and at t_2, respectively. Comparing with the AAVSO lightcurve in Fig. 1, we derive $E_{B-V} = 1.5$ on both such epochs. Taking the unweighted average of all above estimates, the reddening affecting NVul24 is $E_{B-V} = 1.6 \pm 0.1$, which will be adopted in this paper.

The MMRD relation (magnitude at maximum vs. the rate of decline) is frequently used to estimate the distance to a nova. Its most recent formulation by Selvelli & Gilmozzi (2019) is based on Gaia DR2 parallaxes and makes use of t_3 in the V band. The MMRD relation applied to $t_3 = 10.7 \pm 0.5$ days for NVul24 returns an estimated absolute magnitudes $M_V = -8.9 \pm 0.4$, that coupled with $E_{B-V} = 1.6 \pm 0.1$, leads to an estimate of 5 ± 1 kpc as the distance to the nova. A similar distance is derived from the brightness after 15 days (M_{v15}), that was proposed by Buscombe & de Vaucouleurs (1955) to be the same for all novae. The calibration by Selvelli & Gilmozzi (2019) provides $M_{v15} = -5.71 \pm 0.4$ mag, that when applied to NVul24 returns the same 5 ± 1 kpc distance. Such a distance places NVul24 at

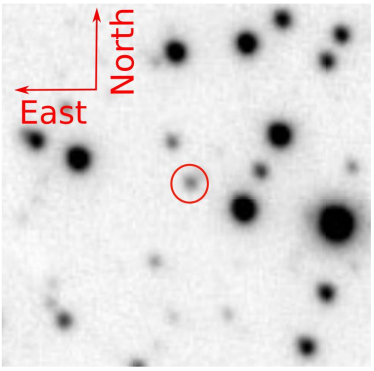

Fig. 3. PanSTARRS r image cropped around the position of NVul24. The size is 30 × 30 arcsec. The red circle has a radius of 1.5 arcsec, and it is centred at the accurate position we measured for NVul24 (cf. Sect. 5). The star close to the centre of the circle is GAIA DR3 1825912166611947136 (of $G = 19.82$ mag), which possibility to be the progenitor of the nova is discussed in Sect. 5.

120 ± 20 pc below the Galactic plane and within the Orion-Cygnus spiral arm.

It should be noted, however, that significant scatter remains in the MMRD M_V and M_{v15} of single novae as already pointed out by Downes & Duerbeck (2000) and also evident in recent surveys on extragalactic novae in M31, M77, M87 (Shara et al. 2017, Shara et al. 2018). It remains unclear whether this scatter arises from intrinsic differences among novae or from observational uncertainties. The main sources of observational uncertainty arise from the determination of reddening along the line of sight, from the accurate measurement of the time of maximum and t_3 which can be affected by undersampling, irregularities, and oscillations in the light curve.

The 5 kpc distance to NVul24 inferred from the MMRD relation is well supported by the reddening progression along the line of sight to the nova, as mapped by the IPHAS (Sale et al. 2014) and Bayestar19 (Green et al. 2019) extinction maps. These maps clearly indicate that a reddening of $E_{B-V} \approx 1.6$ is reached only at distances greater than 4 kpc.

5. Astrometry and identification of the progenitor

The coordinates of NVul24, derived when the nova was close to its peak brightness, have been reported in CBET 5423 as RA = 19:43:07.51, Dec = +21:00:20.4 (J2000.0). In order to check and improve on them, we observed NVul24 on 2024 October 22 when the nova had declined to $V \approx 16$ mag, making the astrometric observations against field stars more robust. To this aim we used the Ferrante 0.36 m telescope operated by Societá Astronomica Schiaparelli in Hakos Farm (Namibia) and the Varese 0.84 m telescope.

Our improved astrometric position for the nova, using the Gaia DR3 catalogue as reference, is RA = 19:43:07.498 and Dec = +21:00:21.23 (0.075 arcsec radius error), and the 1.5 arcsec radius red circle plotted in Fig. 3 is centred on it. A faint star reported both in Gaia DR3 and PanSTARRS DR2 lies within 0.12 arcsec of our position for the nova.

There are pros and cons about considering it the progenitor of NVul24. Let's begin with the problematic aspects.

Gaia DR3 names the star 1825912166611947136 and lists for it $G = 19.82$, $B_P = 20.82$, and $R_P = 18.46$ mag, a slow-moving proper motion, and a parallax $\pi = 1.53 \pm 0.40$ mas (Gaia Collaboration 2016, 2023). Taken at face value, such parallax would suggest a distance ≤1 kpc, much closer than the 5 kpc above estimated for the nova. The associated error (27%) is however too large for an entirely safe inversion of the parallax to derive an accurate value for the distance; to achieve this, Bailer-Jones (2015) and Luri et al. (2018) recommended an error on the parallax that should not exceed 20%.

According to Warner (1995, its Fig. 5.4), there is a good correlation between t_2 and the outburst amplitude for a nova, with faster novae being those showing the largest amplitude. At $G = 19.82$ mag, the candidate progenitor using the geometric parallax distance would imply an outburst amplitude of just ∼11 mag, when the minimum amplitude according to Warner's relation (corresponding to the accretion disk of the progenitor being seen face-on) would be 13 mag.

On the pro side, we note that the Bayesian posterior photogeometric distance estimate from Bailer-Jones et al. (2021), which incorporates colour and magnitude information in addition to the parallax, would give a much larger distance 3.6 kpc, with a 68% confidence interval of 1528–5097 pc.

In addition, PanSTARRS DR2 lists for the star in the circle $g' = 21.50$, $r' = 20.04$, $i' = 19.07$, $z' = 18.55$, and $Y = 18.19$ mag. Correcting them for the reddening affecting the nova ($E_{B-V} = 1.6$ mag) returns an intrinsic rather blue colour $(g - r)_\circ = -0.1$, the same value reported by Inight et al. (2023) as the mean for cataclysmic variables observed by the SLOAN survey. A similar conclusion would be reached by considering Gaia B_P and R_P data.

Moreover, the field around the nova is sparsely populated as illustrated in Fig. 3, and the probability of a chance superposition within ∼0.1 arcsec of a field star with the real progenitor seems improbable, especially considering the rarity of intrinsically blue stars among field objects.

We considered the possibility to invest a sizeable amount of observing time in recording a classification spectrum for the faint star in the circle of Fig. 3, to confirm or disprove it being the progenitor of the nova. We however restrained from that considering that – only one yr past the eruption – the nova ejecta could have not yet diluted sufficiently into the interstellar medium to avoid interfering in the process, especially if the presence of a Hα in emission may be looked for as evidence of accretion being back at work. Waiting a few more years seemed a safer choice.

A fainter Gaia source with $G = 21.01$ mag is located at a distance of 1.1 arcsec from our position of the nova, well outside the astrometric ellipse error. Parallax and proper motion are not available for this star in Gaia DR3.

There is no 2MASS source at the position of NVul24. Around the nova position, the detection of infrared sources appear complete to $J = 16.8$, $H = 15.0$, and $K_s = 14.3$ mag. Adopting colour-dependent reddening relations for the 2MASS system from Fiorucci & Munari (2003), at the distance and reddening above estimated for NVul24, this is equivalent to say that the absolute magnitude of the progenitor is $M(K_s) \geq 0.1$. Comparing with the distribution in $M(K_s)$ of known novae as derived by Munari (2025), this limit is sufficient to exclude the presence of a cool giant or a bright sub-giant as the donor, but leaves ample margins to accomodate a fainter sub-giant. Such a midly evolved companion to the WD, by its intrinsic larger luminosity, would naturally account for the reduced outburst amplitude observed in NVul24.

Summarizing, the main (or better the only) problem with firmly identifying Gaia 1825912166611947136 as the progenitor of NVul24 is the apparently too large Gaia parallax, albeit affected by a significant error, while the intrinsic colour and the

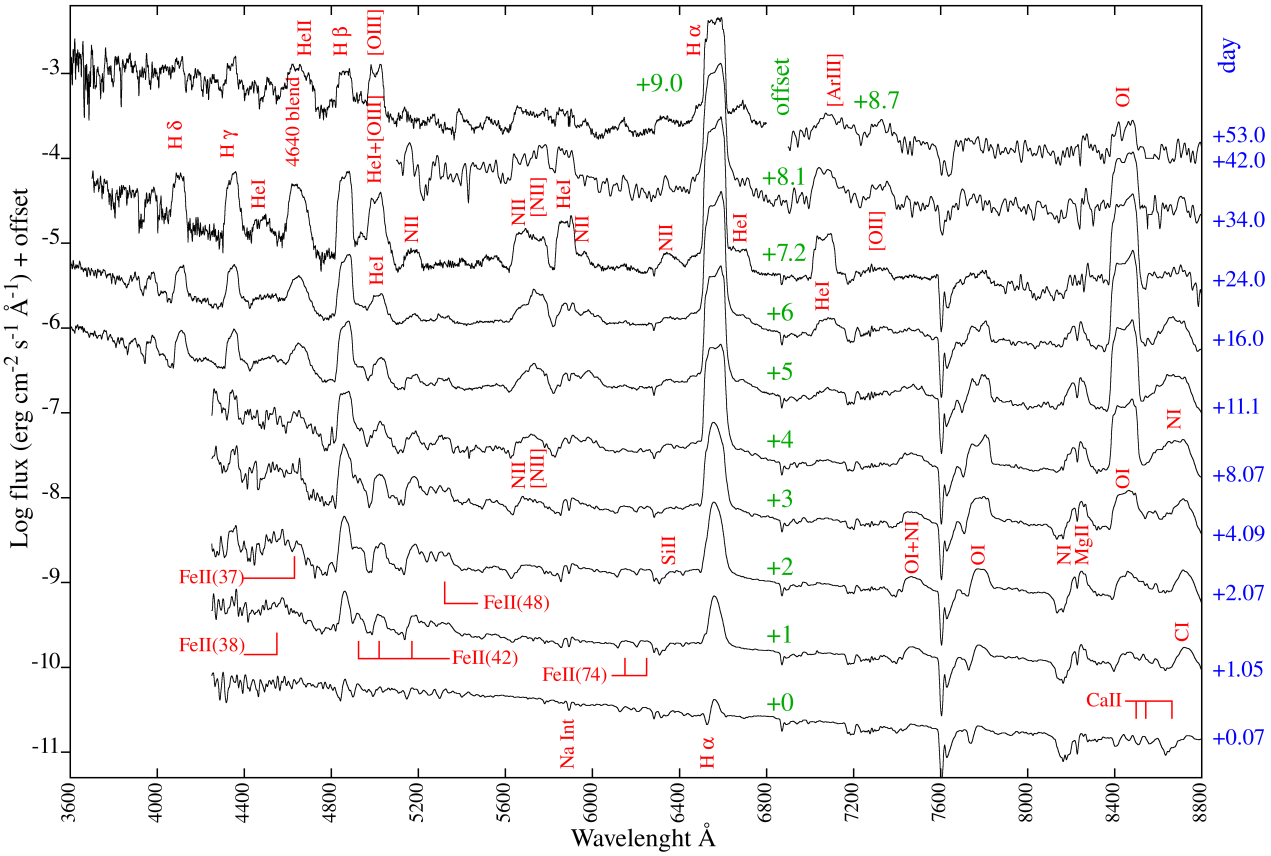

Fig. 4. Spectral evolution of NVul24 for the first 50 days of the outburst. The sequence of sample spectra were obtained in low dispersion with the Asiago 1.22 m + B&C (day +11, +16, +24) and in high resolution with the Varese 0.84 m + Echelle (day +0, +1, +2, +4, +7, +34, +42). The latter were Gaussian smoothed and binned to reduce their spectral resolution to match that of the Asiago 1.22 m + B&C spectra, for an easier intercomparison. The native absolute fluxing of all the spectra has been checked against the AAVSO photometry of Fig. 1, and dereddened by $E_{B-V} = 1.6$. The offset in flux applied to the spectra for a clearer plotting is indicated in green.

spatial coincidence argue strongly in favour, and the oserved outburst amplitude of 11 instead of a minimum of 13 mag can be circumvented by a slightly evolved donor star which presence is compatible with the upper limit to its brightness in the near-IR.

As a final comment, we have accessed the Harvard historical photographic plate collection digitized as part of the DASCH programme (Grindlay et al. 2012), but found no past detection of NVul24, implying that (*i*) no previous nova outburst has been observed, and (*ii*) if the progenitor underwent dwarf-nova outbursts, these were either rather unfrequent or characterized by a low amplitude in brightness (a few magnitudes at most, so that the progenitor remained below the detection threshold of Harvard photographic plates).

6. Spectral evolution

The initial spectral evolution of Nova Vul 2024 up to day +53 is presented in Fig. 4, by combining a sample of spectra selected from those we have recorded (listed in Table A.1).

6.1. Maximum, early decline, and absorption systems

We obtained an echelle spectrum for each of the first five days, during which the changes were most pronounced for this very fast nova. The spectrum of July 30 corresponds to the photometric maximum (day +0.07), dominated by the continuum of the fireball phase. The only lines to appear faintly in emission are Hα, Hβ, OI 7772 and FeII multiplet 42, all accompanied by absorptions on the blue side. The absorption to Hα has a bulk velocity of −1450 km/s and extends to −2270 km/s, values that for OI 7772 turn to −1310 km/s and −2000 km/s, respectively. Blue-shifted absorptions flank also OI 8446, SiII 6347/71, CaII 8252 and the CaII triplet 8498, 8542, 8662 Å.

One day past maximum (our spectrum for day +1.05, cf. Table A.1), as typical for very fast novae, the spectra of NVul24 displayed a retracing continuum and emission lines of increasing flux, very broad and flanked by weakening P-Cyg absorptions. The OI 7772, 8446 and the FeII emission lines (multiplets 37, 38, 42, 48 and 74) gave to NVul24 spectra the aspect typical of FeII-class novae following the classification by Williams (1992). The equivalent width of Hα increased from −25 Å on day +0.07 to −158 Å on day +1.05 (see also Fig. 1), when it displayed a FWHM = 2470 km/s. The broad blue-shifted absorption to Hα became narrower and moved to −1720 km/s, with possible secondary components at −1250 and −2200 km/s. They can be identified with the principal absorption system according to the nomenclature of McLaughlin (1960). At the same time, the broader diffuse enhanced absorption system also appeared, centred at −2800 km/s and extending up to −3500 km/s at about twice the average velocity of the principal absorption. A detailed description of the evolution of absorptions systems for Hα for the first three days is provided in Appendix C.

The strong emission seen during the first three days around 8725 Å may be identified with CI 8727 Å, following

Della Valle et al. (2002). Other strong emission features in the red appears to originate from blends: that at 8650 should come from multiplets #6 of SI and #1 of NI, at 8220 Å between multiplets #2 of NI and #7 of MgII, that at 7477 from multiplets #3 of NI and #55 of OI. In Fig. 4 the feature at 8220 Å displays an apparently double-peaked profile, but this is a spurious effect caused by the superposition of a strong telluric absorption and an Echelle inter-order gap (8239–8246 Å).

6.2. Hα and OI 8446 Å evolution

The evolution in flux and profile of Hα and OI 8446 Å line is presented in parallel in Fig. 5.

Around the passage at t_2 on day +5, the shape of Hα changed from a rounded profile to a "wedding cake" arrangement, with a rectangular pedestal of FWHM = 4300 km/s and a superimposed narrower component of FWHM = 2750 km/s. The boxy pedestal to Hα turns visible at the same time the broken power-law of Fig. 2 enters the $\alpha = -1.48$ branch, which according to Hachisu & Kato (2006) should mark the transition from optically thick to thin conditions in the wind that they propose blows off the WD of novae during their early evolution. The Hα pedestal freezed its profile to FWHM = 4300 km/s and FWZI = 5800 km/s for the rest of the nova evolution past t_2. Williams (1992) sub-divided the FeII class of novae based on the value of FWZI, with 5000 km/s separating the FeIIb (for 'broad') from the FeIIn (for 'narrow') types. At FWZI = 5800 km/s NVul24 belongs to the FeIIb novae, which Williams (1992) noted are the best candidates to become hybrid novae.

Starting from day +2 and up to day +30, OI 8446 Å became the second most intense emission line after Hα, with a similar profile and the same width. From day +7 to day +21 the dereddened intensity of OI 8446 Å line remained at around 25% of Hα. The intensity of 8446 Å triplet OI line, under pure recombination and optically thin conditions, should be 3/5 of the quintuplet OI 7773 Å line, but the dereddened flux ratio 8446/7773 in NVul24 reached ∼30 by day +25 and was still ≥10 in the spectrum for day +25 when the 7773 Å line was last visible.

The inversion in intensity between these two OI lines in novae ejecta is usually attributed to Lyman-β fluorescence pumping of the OI 8446 Å line, as first described by Bowen (1947). Lyman-β photons can be generated in regions where neutral Oxygen is abundant, through the conversion of Hα photons, provided that the $n = 2$ levels of HI are significantly populated by collisions (Strittmatter et al. 1977). Such regions, with locally high opacity in Hα, can be identified with dense discrete blobs of gas embedded in the thin wind of the ejecta. The Doppler signature of their differing radial velocities is confirmed by the castellated shape of the Hα profile shown in Fig. 8.

6.3. Emergence of He/N spectrum and hybrid classification

A striking feature of Fig. 4 is the emergence around day +7 of the NII+OII+NIII blend at 4640 Å as well as the [NII] 5755 + NII 5678 and NII 5938 + HeI 5876 blends. They are typical of the He/N class of novae (Williams 1992).

As the FeII lines progressively weaken from day +11 onwards, the spectrum of a He/N-type nova begins to emerge, becoming fully developed between days +16 and +24. A comparison of the spectrum of NVul24 for day +16 with those of the hybrid nova V5588 Sgr and the He/N nova KT Eri is presented in Fig. 6. There are only very few novae that have been seen to evolve from a FeII- to an He/N-type spectrum or to have

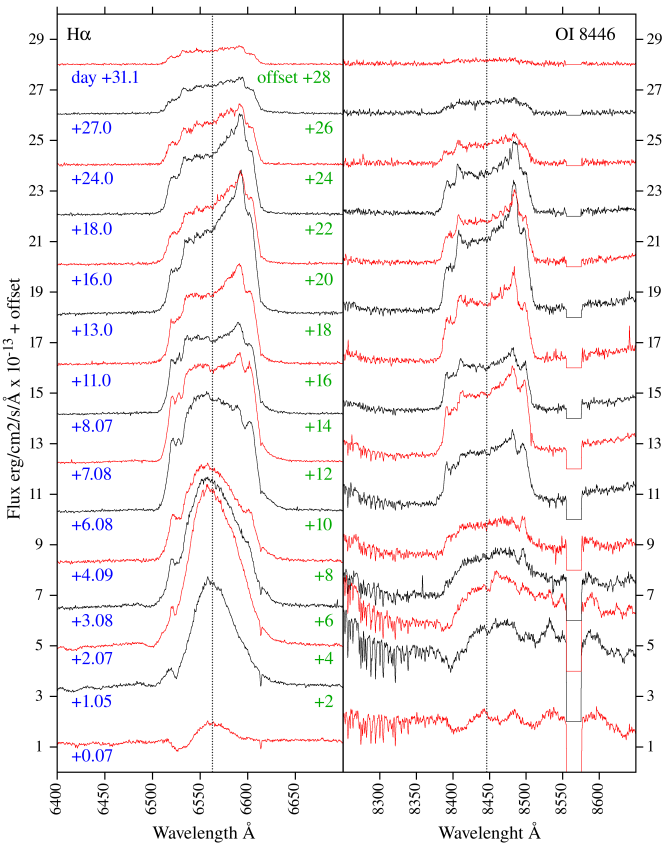

Fig. 5. Evolution of Hα, and OI 8446 Å emission lines. The Hα line profile has been corrected for telluric absorbptions. No correction was applied to OI 8446 Å line because telluric absorptions ends redward 8377 Å. The drop in intensity between 8555 and 8575 Å is artificial and represents an inter-order gap in the Echelle spectra.

simultaneously shown them both. Williams (1992) called them "hybrid" novae and defined them as "novae that change between the two spectral classes during the early permitted emission-line phase, evolving from an FeII type spectrum to that of a He/N type spectrum before forbidden lines appear".

The nature of the hybrid spectra observed in some novae remains debated. Williams (2012) suggested that the physical conditions producing He/N spectra are consistent with an origin in the white dwarf (WD) ejecta, whereas Fe II spectra arise in an extended circumbinary gas envelope, likely originating from the secondary star. In hybrid novae, the transition between the two spectral classes is attributed to the temporal evolution of the physical parameters in these two emitting regions during the post-outburst decline.

More recently, Aydi et al. (2024) proposed that all novae experience an initial He/N phase during the rise to maximum light, followed by an Fe II phase and a second He/N phase prior to the onset of the nebular spectrum. In this framework, the observed spectral class depends primarily on the opacity and ionization state of the ejecta. However, one of these phases may frequently remain unobserved because of its short duration.

We present a detailed spectroscopic description of the Fe II–to–He/N transition in NVul24, with the aim of contributing to a clearer understanding of the scenario underlying its occurrence. Other recent examples of genuinely hybrid novae are V1674 Her (Woodward et al. 2021), V5588 Sgr (Munari et al. 2015), V5114 Sgr (Anupama 2012), and V458 Vul (Poggiani 2008a). A list complete to the best of our knowledge is provided in Table 1.

Table 1. List of genuine hybrid novae.

Name	Year	t_2	Oscillations	[OI]	Neon overabund.	Reference
V615 Vul	2024	5	yes	no		this paper
V1674 Her	2021	1	no	no	yes	Woodward et al. (2021)
V5588 Sgr	2011	38	6 secondary maxima	no		Munari et al. (2015)
V458 Vul	2007	7	yes	no	yes?	Poggiani (2008b)
M31N 2006-10b	2006	≈11		no		Shafter et al. (2011)
V5114 Sgr	2004	11	no	yes	yes	Ederoclite et al. (2006)
V444 Sct	1991	6		no	yes	Williams et al. (1994)
V838 Her	1991	≈4	no	no	yes	Williams et al. (1991)
LMC 1988-2	1988			no		Williams et al. (1991)

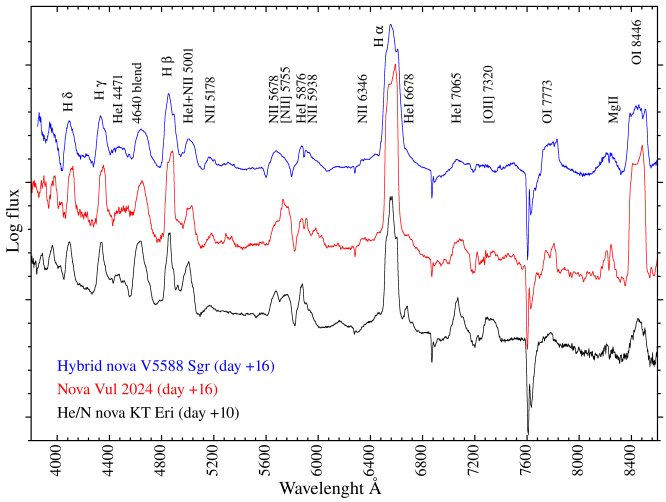

Fig. 6. Spectrum of NVul24 for day +16, compared to those of the hybrid nova V5588 Sgr and the He/N nova KT Eri.

Williams et al. (1991) intially considered the symbiotic recurrent nova V3890 Sgr as an example of hybrid novae, but as clearly revealed by the intensive spectral monitoring of its latest outburst in 2019 (e.g. Sims 2020; Page et al. 2020, among many others), the nova spectrum is of the He/N type since the beginning, with FeII features arising in the ionized wind of the late type giant and not in the ejecta, (see Sect. 3.1 of Munari 2025), and therefore there is no relation of V3890 Sgr to real hybrid novae or classical novae at large.

Due to the large width and consequent strong blend of the emission lines, it is not possible to easily isolate the lines associated with the He/N-class spectrum and compare their Doppler profile with those of the FeII-class spectrum, in order to derive expansion velocities and the geometry of the ejecta for each system. What is certain is that the strong asymmetry affecting Hα between days +13 and +18 (cf. Fig. 5) does not replicate in the profile of NII 5001 Å.

Novae of the FeIIn type usually display significant [OI] 5755, 6300, and 6364 emission lines, which persist even when the spectrum of the nova turns to high ionization condition (such as [CaV] or [FeVII] emission lines). Williams (1994) evaluated the optical thickness in the [OI] lines, their collisional excitation, and shielding from the hard ionizing photons permeating the ejecta, concluding they can only form in isolated, small and dense blobs/condensations expanding alongside with the much lower density general ejecta. Interestingly, there are no clearly visible [OI] lines in the spectra of NVul24, and absence or great weakness of [OI] lines is the hallmark of hybrid novae (cf. Table 1), reinforcing the partneship of NVul24 with them.

6.4. Spectroscopic behaviour during photometric oscillations

The appearance of the He/N spectrum in NVul24 overlaps with the onset of photometric oscillations, whose maxima occurred on days +14, +20, +26, +32, +42, +52, and +63, the latter two values being rather uncertain given the large noise affecting the AAVSO-based light curve of Fig. 1. There seems to be no direct relation between NVul24 turning hybrid and the appearance of the oscillations, and no such a correlation may be clearly established for the other hybrid novae listed in Table 1.

The first (maximum on day +14) and the third (maximum on day +26) oscillation have been covered by our spectral observations, with spectra available at maximum and at the preceding minimum (indicated by the arrows in Fig. 1). The spectra at minimum and maximum, and their subtraction differences, are compared in Fig. 7. In both cases the increase in nova brightness appears primarily driven by a continuum turning brighter, in agreement with the fact that the oscillations are similarly well visible in all the *BVRI* bands (see Fig. B.1). From the top two panels of Fig. 1, it is rather evident how Hα emission passed unscathed through the oscillations, while the continuum-dominated Stromgren *y* band show the first oscillations amplified compared to *BVRI* bands.

The difference spectrum in Fig. 7 clearly indicates how the oscillation on day +14 is accompanied by a flux increase of the emission lines associated with the He/N spectrum, while little or no variation observed for FeII and Balmer lines. A careful inspection of the line shape in the subtracted spectrum suggests also an asymmetric enhancement for the HeI lines, with the red part of the profile turning stronger. The same behaviour affects Hα that simultaneously with the oscillation developed a peak at +1400 km/s (cf. Fig. 5). The +1400 km/s Hα peak remained correlated with the photometric behaviour on the following days: it decreased on day +16 (close to photometric minimum), strengthened again on day +18 (close to second oscillation maximum of day +20) and decreased once more by day +24 (near another minimum).

The difference spectrum for the day +26 oscillation (the third one) tells however the reverse story compared to day +14 oscillation, as it is well visible in Fig. 7. This time it is the He/N spectrum that weakens with the rise to peak brightness of the oscillation, expecially the NII lines, with a parallel large surge in the emission of forbidden lines such as [NII] 5755, [ArIII] 7136, and [OII] 7325, and the possible reappeance of FeII again in emission. Another significant difference compared to the oscillation

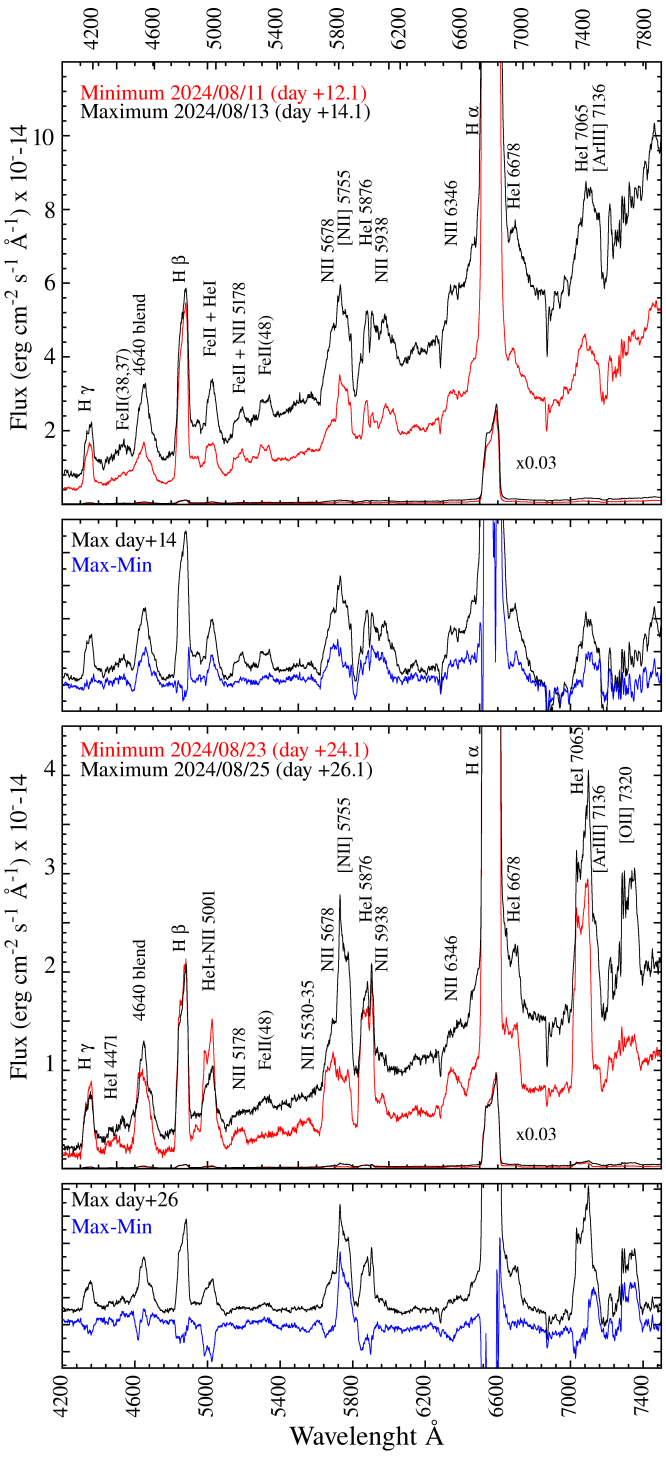

Fig. 7. Spectral evolution through oscillations. Large panels: Absolutely fluxed spectral evolution between maxima (black) and minima (red) across the first and third pscillations. To show the evolution of Hα, the same spectra are also superimposed reduced by a factor of 50. Small panels: difference spectrum (blue) between continuum subtracted spectra at maximum and at minimum, compared to the spectrum at maximum (black).

on day +14 is the absence of any enhancement of the +1400 km/s peak in the Hα profile with the passage at maximum brightness.

We recorded Echelle spectra also near the minimum and maximum of the oscillation of day +42 (the fifth of the series). By that time the brightness of the nova had already declined to $V \approx 14$, and the high-resolution Echelle spectra were affected by a low S/N. Nonetheless, also for this oscillation an increase in the forbidden lines [NII] 5755, [ArIII] 7136 and [OII] 7325 Å is observed near maximum brightness.

In light of their spectroscopic evolution, the nature of the photometric oscillations in NVul24 appear to differ from those sometimes observed in slow novae, where the spectra around maximum show broadening of the emission lines – possibly accompanied by high-velocity P Cygni absorptions and lower ionization conditions – as reported for V1405 Cas (Valisa et al. 2023), V5558 Sgr (Poggiani 2008a) and V4745 Sgr (Csák et al. 2005). Nor can the oscillations in NVul24 be compared to the flares occasionally observed during the nebular phase, which typically involve intensity variations in high-ionization lines such as [FeVII] and [FeX], such as those described by Munari et al. (2022) for Nova Sct 2019 or Di Giacomo et al. (2025) for Nova Cas 2021.

It appears relevant to note that the onset of the oscillations of NVul24 coincides with the detection of X-rays with the Swift satellite as reported by Sokolovsky et al. (2024a). The hard spectrum of the X-rays suggest an origin in shock-heated plasma. The Swift/XRT count rate peaked on day +16 at 0.068 ± 0.011 cts/s and declined to 0.042 ± 0.006 by day +24. The transition of NVul24 to nebular conditions, with the emergence of [OIII] lines, also occured during the final stages of the oscillations season. The potential connection between the observed oscillations and shock-driven X-ray emission is intriguing; however, the sparse X-ray data available in the literature for this source limits further discussion to a speculative level, making a more quantitative analysis currently unfeasible.

6.5. The nebular phase

In the spectrum of day +53, shown at the top of Fig. 4, the intensity of [OIII] 5007 finally exceeded that of Hβ, marking the onset of the nebular phase, which occured when the V-band luminosity of NVul24 had declined 5 magnitudes below maximum. The reduction in density and transition to optically thin condition in the ejecta led to a significant decrease in the Lyman-β fluorescence of the OI 8446 line, while the increasing ionization favoured HeII over HeI, with HeII becoming visible on the red side of the 4640 Å blend.

Despite the ionization conditions at this stage being favourable for the excitation of [NeIII], no trace of [NeIII] 3869, 3968 lines was observed in the spectrum recorded on day +53, or in the subsequent spectra taken on days +91 and +107 (Fig. 8), when the V-band magnitude had already declined to $V = 16.5$ and $V = 17$ respectively. The very red colour and overall faintness prevented us from reaching down to [NeV] 3427. The absence of emission in Ne lines indicates that NVul24 is not a neon nova. We have extensively experimented with the photoionization code Cloudy v23.01 (Gunasekera et al. 2023) for the physical conditions of NVul24; for the typical overabundance of neon novae, the [Ne III] 3869 line would be expected to be significantly more intense than both [O III] 4363, 5007 and Hβ, while a Solar abundance agrees with the lack of detection.

Our last spectrum was secured on day +118, with medium dispersion (0.6 Å/pix) allowing a comparison of the Hα profile with that recorded at the beginning of the nebular phase on day +53 (cf. Fig. 8). The two profiles are very similar indicating that the ejecta were expanding in a balistic way into the surrounding space; the minor changes visible in the peaks of the jagged top, can be ascribed to the low S/N of the later spectrum.

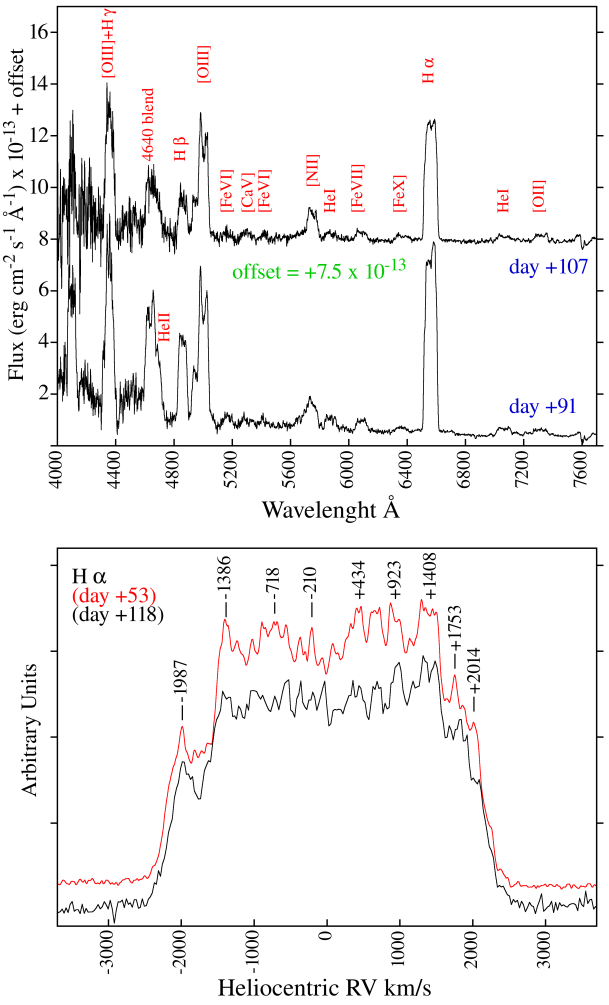

Fig. 8. Spectra during nebular phase. Upper panel: reddening-corrected spectra to highlight the evolution of NVul24 during the advanced nebular stage. Lower panel: comparison of the Hα profiles for day +53 and +118, with indication of the velocity (in km/s) for some features.

On day +118, the Hα profile exhibits a trapezoidal base with FWHM = 4340 km/s (FWZI = 5030 km/s) upon which a second boxy and castellated emission component with FWHM = 3130 km/s is superimposed. Although an analysis of the shape of the ejecta is beyond the scope of this paper, a similar structure has been modelled for ejecta composed of equatorial rings and polar caps (Ribeiro et al. 2011; Gill & O'Brien 1999). The spectra from days +91 and +107 show the evolution towards lower-density conditions resulting in an increase in forbidden line intensities relative to permitted one, alongside a decrease in the Balmer lines, HeI lines and 4640 Å blend. In the dereddened spectra from day +107, shown in the Fig. 8, the blend of [OIII] 4959+5007 Å reaches the intensity of Hα and [OIII] 4363 Å is perhaps even stronger. The overall spectral evolution aimed to higher ionization conditions, culminating in the probable appearance (although at low flux) of [FeX] on the latest spectrum for day +107.

7. Conclusions

We have performed extensive spectroscopic monitoring of Nova Vul 2024, from its passage at optical maximum to well into the nebular stage and the appearance of the coronal [FeX] line.

Table 2. Summary of the main parameters for Nova Vul 2024.

coordinates = 19:43:07.498, +21:00:21.23 (±0.075 arcsec)
galactic coord. = 57.4084, −1.2801
t_{max} = 2460522.3 HJD (2024 July 30.8 UT)
V_{max} = 9.6 mag
type = initial FeII, then hybrid
t_2 = 5 ± 0.5 days
t_3 = 10.7 ± 0.5 days
E_{B-V} = 1.6 ± 0.1 mag
M_V = −8.9 ± 0.4 mag (from MMRD)
distance = 5 ± 1 kpc (from MMRD)
FWZI(Hα) = 5800 km/s
probable
progenitor = Gaia DR3 1825912166611947136

Supported by available AAVSO and ZTF photometry, we have derived the primary properties of this very fast and highly reddened nova, which turned out to be a member of the rare class of hybrid novae.

Both the decline time t_3 = 10.7 days and the E_{B-V} = 1.6 reddening were robustly determined; the application of the MMRD relation to them provided a distance to the nova of ≈5 kpc, in fine agreement with 3D maps of the extinction through the Galaxy. For the line of sight to the nova, these maps imply a lower limit of 4 kpc to the distance.

We obtained refined astrometry of the nova during the advanced nebular stage, which led to a robust positional match with a G = 19.8 mag star present in both the Gaia and PanSTARRS catalogues. While the Gaia parallax is inconclusive, the blue colour of this field star, as registered by both Gaia and PanSTARRS, matches the typical colour of nova progenitors. The lack of a 2MASS counterpart excludes a giant or a bright sub-giant as the donor star in the progenitor, while a faint sub-giant would naturally explain the somewhat reduced outburst amplitude for NVul24.

The spectrum of the nova around maximum was typical of the FeII-class, with very broad emission lines (FWZI ∼ 5800) and high-velocity P-Cyg absorption reaching terminal velocities ≈−3500 km s^{-1}. After t_3, the nova began experiencing photometric oscillations primarily driven by changes in the continuum and the emergence of hard X-ray emission, while emission lines typical of the He/N-class began to develop in parallel to those of the FeII-class, characterizing NVul24 as a member of the rare class of hybrid novae.

During the nebular phase, up to the last spectrum obtained at day +118, the ejecta remained at relatively high densities; the ionization kept increasing, passing through [FeVII] and probably up to [FeX]. The ejecta did not show overabundance in neon, and for most of the monitored time, they expanded in a simple ballistic pattern, as demonstrated by the width, profile, and castellation of the high-resolution emission-line profiles. A summary of the main parameters for Nova Vul 2024 is reported in Table 2.

Data availability

The spectral data presented in this work were obtained by the authors and are available at the CDS via https://cdsarc.cds.unistra.fr/viz-bin/cat/J/A+A/707/A326

Photometric data from AAVSO and ZTF are publicly available and can be accessed directly through their respective web portals.

Acknowledgements. We would like to thank the anonymous referee for the valuable comments that helped to improve the paper and clarify its content. We also express our gratitude to L. Buzzi for performing accurate astrometry of NVul24 and A. Milani for downloading hystorical DASCH data. We acknowledge the variable star observations from the AAVSO International Database contributed by observers worldwide and used in this research. This work has been in part supported by INAF 2023 MiniGrant Programme (contract C93C23008470001 to UM). The ZTF forced-photometry service was funded under the Heising-Simons Foundation grant 12540303 (PI: Graham).

References

Anupama, G. C. 2012, Astron. Soc. India Conf. Ser., 6, 143
Aydi, E., Chomiuk, L., Strader, J., et al. 2024, MNRAS, 527, 9303
Azzollini, A., Shore, S. N., Kuin, P., & Page, K. L. 2023, A&A, 674, A139
Bailer-Jones, C. A. L. 2015, PASP, 127, 994
Bailer-Jones, C. A. L., Rybizki, J., Fouesneau, M., Demleitner, M., & Andrae, R. 2021, AJ, 161, 147
Bowen, I. S. 1947, PASP, 59, 196
Buscombe, W., & de Vaucouleurs, G. 1955, Observatory, 75, 170
Craig, P., Aydi, E., Chomiuk, L., et al. 2025, MNRAS, 538, 2339
Csák, B., Kiss, L. L., Retter, A., Jacob, A., & Kaspi, S. 2005, A&A, 429, 599
Della Valle, M., Pasquini, L., Daou, D., & Williams, R. E. 2002, A&A, 390, 155
Di Giacomo, R., Shore, S. N., Munari, U., et al. 2025, A&A, 703, A238
Downes, R. A., & Duerbeck, H. W. 2000, AJ, 120, 2007
Ederoclite, A., Mason, E., Della Valle, M., et al. 2006, A&A, 459, 875
Fiorucci, M., & Munari, U. 2003, A&A, 401, 781
Gaia Collaboration (Prusti, T., et al.) 2016, A&A, 595, A1
Gaia Collaboration (Vallenari, A., et al.) 2023, A&A, 674, A1
Gill, C. D., & O'Brien, T. J. 1999, MNRAS, 307, 677
Green, G. M., Schlafly, E., Zucker, C., Speagle, J. S., & Finkbeiner, D. 2019, ApJ, 887, 93
Grindlay, J., Tang, S., Los, E., & Servillat, M. 2012, IAU Symp., 285, 29
Gunasekera, C. M., van Hoof, P. A. M., Chatzikos, M., & Ferland, G. J. 2023, Res. Notes Am. Astron. Soc., 7, 246
Hachisu, I., & Kato, M. 2006, ApJS, 167, 59
Hachisu, I., & Kato, M. 2007, ApJ, 662, 552
Hachisu, I., Kato, M., Kiyota, S., et al. 2008, ASP Conf. Ser., 401, 206
Iijima, T., & Naito, H. 2011, A&A, 526, A73
Inight, K., Gänsicke, B. T., Breedt, E., et al. 2023, MNRAS, 524, 4867
Kiss, L. L., & Thomson, J. R. 2000, A&A, 355, L9
Kiss, L. L., Gogh, N., Vinkó, J., et al. 2002, A&A, 384, 982
Kos, J., & Zwitter, T. 2013, ApJ, 774, 72
Luri, X., Brown, A. G. A., Sarro, L. M., et al. 2018, A&A, 616, A9
Masci, F. J., Laher, R. R., Rusholme, B., et al. 2019, PASP, 131, 018003
McLaughlin, D. B. 1960, in Stellar Atmospheres, ed. J. L. Greenstein (Univ. of Chicago Press), 585
Munari, U. 2014, ASP Conf. Ser., 490, 183
Munari, U. 2025, CAOSP, 55, 47
Munari, U., & Valisa, P. 2014, CAOSP, 43, 174
Munari, U., & Zwitter, T. 1997, A&A, 318, 269
Munari, U., Henden, A., Banerjee, D. P. K., et al. 2015, MNRAS, 447, 1661
Munari, U., Righetti, G. L., & Dallaporta, S. 2022, MNRAS, 516, 4805
Page, K. L., Kuin, N. P. M., Beardmore, A. P., et al. 2020, MNRAS, 499, 4814
Poggiani, R. 2008a, New Astron., 13, 557
Poggiani, R. 2008b, Ap&SS, 315, 79
Poggiani, R. 2009, Astron. Nachr., 330, 77
Ribeiro, V. A. R. M., Darnley, M. J., Bode, M. F., et al. 2011, MNRAS, 412, 1701
Sale, S. E., Drew, J. E., Barentsen, G., et al. 2014, MNRAS, 443, 2907
Schwarz, G. J., Ness, J.-U., Osborne, J. P., et al. 2011, ApJS, 197, 31
Selvelli, P., & Gilmozzi, R. 2019, A&A, 622, A186
Shafter, A. W., Darnley, M. J., Hornoch, K., et al. 2011, ApJ, 734, 12
Shara, M. M., Doyle, T., Lauer, T. R., et al. 2017, ApJ, 839, 109
Shara, M. M., Doyle, T. F., Pagnotta, A., et al. 2018, MNRAS, 474, 1746
Sims, F. 2020, 39th Annual Conference of the Society for Astronomical Sciences (SAS-2020), 199
Sokolovsky, K., Aydi, E., Chomiuk, L., et al. 2024a, ATel, 16788, 1
Sokolovsky, K., Aydi, E., Chomiuk, L., et al. 2024b, ATel, 16751, 1
Sokolovsky, K., Korotkiy, S., Potapov, N., et al. 2024c, CBETs, 5423, 1
Strittmatter, P. A., Woolf, N. J., Thompson, R. I., et al. 1977, ApJ, 216, 23
Strope, R. J., Schaefer, B. E., & Henden, A. A. 2010, AJ, 140, 34
Taguchi, K. 2024, ATel, 16743, 1
Valisa, P., & Munari, U. 2024, ATel, 16746, 1
Valisa, P., Munari, U., Dallaporta, S., Maitan, A., & Vagnozzi, A. 2023, ArXiv e-prints [arXiv:2302.04656]
van den Bergh, S., & Younger, P. F. 1987, A&AS, 70, 125
Warner, B. 1995, Cataclysmic Variable Stars (Cambridge Univ. Press), 28
Williams, R. E. 1992, AJ, 104, 725
Williams, R. E. 1994, ApJ, 426, 279
Williams, R. 2012, AJ, 144, 98
Williams, R. E., Hamuy, M., Phillips, M. M., et al. 1991, ApJ, 376, 721
Williams, R. E., Phillips, M. M., & Hamuy, M. 1994, ApJS, 90, 297
Woodward, C. E., Banerjee, D. P. K., Geballe, T. R., et al. 2021, ApJ, 922, L10

Appendix A: Journal of spectroscopic observations of Nova Vul 2024.

We report in the table below a journal of the spectroscopic observations of NVul24 that we have recorded at the Varese and Asiago observatories.

Table A.1. Log book of spectroscopic observations of Nova Vul 2024.

date	HJD	t-t_0 (days)	expt (sec)	disp. (Å/pix)	res.pow. $\lambda/\Delta\lambda$	λ range (Å)	tel.
2024-07-30	2460522.38	0.07	2700		10000	4250-8900	0.84m
2024-07-31	2460523.35	1.05	2700		10000	4250-8900	0.84m
2024-08-01	2460524.37	2.07	2700		10000	4250-8900	0.84m
2024-08-02	2460525.38	3.08	1800		10000	4250-8900	0.84m
2024-08-03	2460526.39	4.09	2400		10000	4250-8900	0.84m
2024-08-05	2460528.38	6.08	2700		10000	4250-8900	0.84m
2024-08-06	2460529.38	7.08	2700		10000	4250-8900	0.84m
2024-08-07	2460530.37	8.07	2700		10000	4250-8900	0.84m
2024-08-09	2460532.35	10.1	1500	2.3		3317-7880	1.22m
2024-08-10	2460533.33	11.0	2700		10000	4250-8900	0.84m
2024-08-10	2460533.36	11.1	1800	2.3		3317-7880	1.22m
2024-08-11	2460534.43	12.1	2400	2.3		3317-7880	1.22m
2024-08-12	2460535.33	13.0	2700		10000	4250-8900	0.84m
2024-08-13	2460536.45	14.1	2400	2.3		3317-7880	1.22m
2024-08-15	2460538.37	16.0	2700		10000	4250-8900	0.84m
2024-08-15	2460538.46	16.1	2400	2.3		3317-7880	1.22m
2024-08-16	2460539.47	17.1	2400	2.3		3317-7880	1.22m
2024-08-17	2460540.37	18.0	2700		10000	4250-8900	0.84m
2024-08-22	2460545.39	23.0	2400	2.3		3317-7880	1.22m
2024-08-23	2460546.32	24.0	3600		10000	4250-8900	0.84m
2024-08-23	2460546.38	24.1	3600	2.3		3317-7880	1.22m
2024-08-25	2460548.45	26.1	3600	2.3		3317-7880	1.22m
2024-08-26	2460549.37	27.0	2700		10000	4250-8900	0.84m
2024-08-30	2460553.40	31.1	3600		10000	4250-8900	0.84m
2024-09-02	2460556.36	34.0	3600		10000	4250-8900	0.84m
2024-09-06	2460560.37	38.0	3600		10000	4250-8900	0.84m
2024-09-10	2460564.36	42.0	3600		10000	4250-8900	0.84m
2024-09-21	2460575.35	53.0	1200		23000	3485-7135	1.82m
2024-10-29	2460575.35	91.0	3600	2.3		3317-7880	1.22m
2024-11-15	2460630.21	107.9	3600	2.3		3317-7880	1.22m
2024-11-25	2460640.21	117.9	3600	0.6		5770-7000	1.22m

Notes. The interval $t - t_0$ is counted from the epoch of maximum optical brightness on 2024 Jul 30.8 UT (HJD=2460522.3). The last column identifies the telescopes: Varese 0.84m, Asiago 1.22m, and Asiago 1.82m.

Appendix B: BVRI photometry

Photometry evolution of NVul24 using B, V, R, and I observations from AAVSO (binned to half a day interval to reduce noise) and ZTF g and r data.

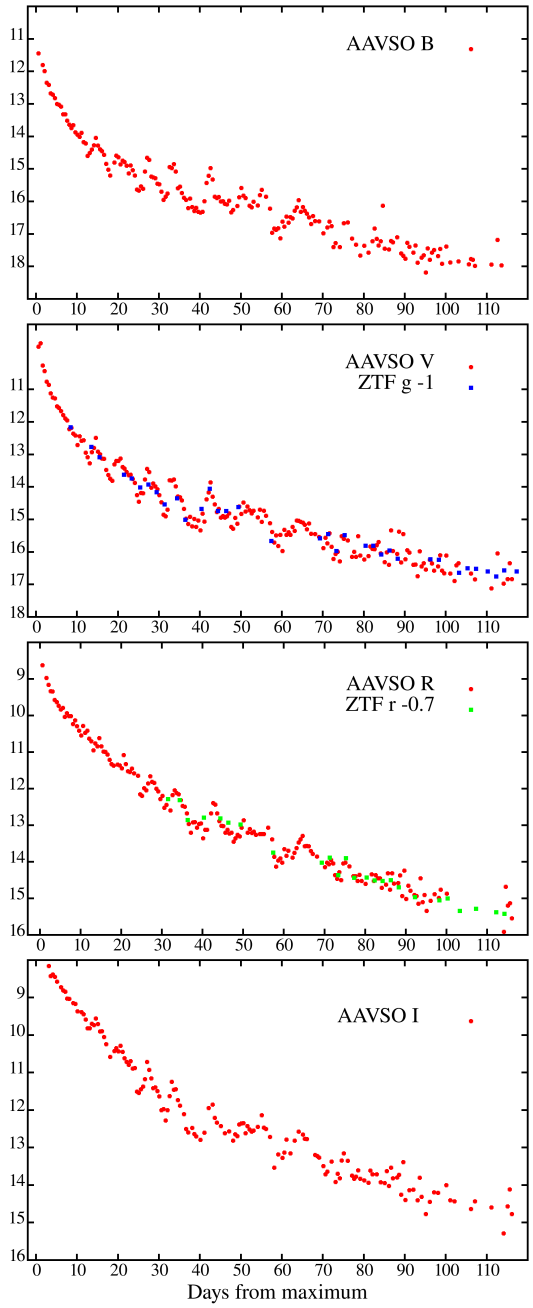

Fig. B.1. B, V, R, and I band light-curves of Nova Vul 2024. Red dots are from the AAVSO database, binned to half a day to reduce the noise. Blue dots are ZTF g magnitudes shifted to V band by adding a -1 mag offset, while green dots are ZTF r magnitudes shifted to R band by adding a -0.7 mag offset. The earliest three measurements in the V-band panel, covering the rise to maximum, have been imported from CBET 5423. The observing epochs are counted as days passed since optical maximum on 2024 Jul 30.8 UT (HJD=2460522.3).

Appendix C: Evolution of Principal and Diffuse Enhanced absorption systems

As expected for a very fast nova, the spectral changes of NVul24 in the first few days after discovery were very rapid, and the "principal" and "diffuse enhanced" absorptions systems for Hα (cf. McLaughlin 1960), can be followed only for the first three days past maximum. They are shown in Fig. C.1 and measured Table C.1 below. From day +4 the principal absorption system merged with the shoulder of the developing boxy profile of Hα, as visible in Fig. 5 .

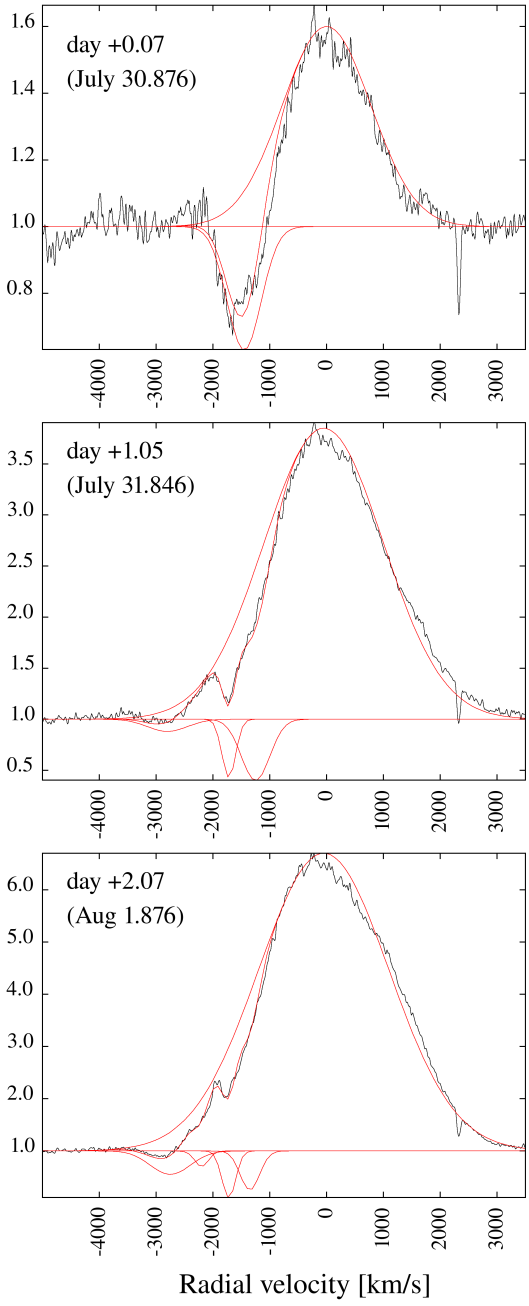

Fig. C.1. Continuum normalized Hα profiles of Nova Vul 2024 for the first three days past maximum. The observed spectrum is shown in black, whereas the overall fit and the individual components are shown in red. Their parameters are reported in Table C.1.

It is worth noticing that the velocities reported in Table C.1 well conform with the value predicted by the relations calibrated by (McLaughlin 1960) against t_3:

$$\log V_p = 3.70 - 0.5 \cdot \log t_3 = 1513 \text{ km/s} \quad \text{(C.1)}$$

$$\log V_{DE} = 3.81 - 0.4 \cdot \log t_3 = 2511 \text{ km/s} \quad \text{(C.2)}$$

Considering that the (vast) majority of the novae used by (McLaughlin 1960) to calibrate these relations were of the FeII type (a classification not known at the time being introduced only much later by Williams (1992)), the agreement with the velocities measured on our programme nova support the notion that - even if turning hybrid at a later time - NVul24 was initially behaving like a standard FeII nova, including the structure and velocity of P-Cyg absorption systems.

Table C.1. Components of the Hα line profile of Nova Vul 2024.

date (2024)	$RV_\odot$ (km/s)	WHM (km/s)	e.w. (Å)	Flux	System
day +0.07	0	915	−24.7	25	*em.*
(Jul 30.876, UT)	−1450	350	5.9	5.9	*P*
day +1.05	−50	1235	−158	93	*em.*
(Jul 31.846, UT)	−1250	140	3.6	2.1	*P*
	−1720	290	7.9	4.6	*P*
	−2800	410	2.2	1.3	*DE*
day +2.07	−50	1350	−346	127	*em.*
(Aug 1.876, UT)	−1350	200	6.7	2.5	*P*
	−1720	140	5.7	2.1	*P*
	−2200	140	1.9	0.7	*P*
	−2750	410	8.3	3.0	*DE*

Notes. WHM denotes the width at half maximum; "em" is the emission component, "P" and "DE" are the principal and diffuse-enhanced absorption systems, respectively. The flux is expressed in units of 10^{-12} erg cm^2 s^{-1} .

Appendix D: Dereddened fluxes of emission lines observed in the spectra of NVul24 for days +91 and +107.

Our latest full-range spectra of NVul24 were obtained on 2024 Oct 29 and Nov 15 (day +91 and +107), and are visible in the top panel of Fig. 8 after correction for the E_{B-V}=1.6 mag reddening. They have been recorded when the dilution of the ejecta conformed to optically thin conditions over the bulk of their mass. We report in the table below the integrated flux of the most relevant emission lines of NVul24 that we have measured on these spectra. For the 4640+HeII 3686 and [OIII] 4959+5007 blends, we assumed the same profile for each contributing line, and adjusted the relative fluxes by χ^2 fitting to the overall blend profile. That is not possible for Hγ+[OIII] 4363 which are almost exactly superimposed.

Table D.1. Dereddened fluxes of emission lines observed in the spectra of NVul24 for days +91 and +107.

Name	Wavelength (Å)	Flux ($\times 10^{-12}$ erg cm^2 s^{-1}) day +91	day +107
[NeIII]	3869	< 10	< 5
Hδ	4102	20.0	6.0
[OIII] + Hγ	4363-40	38.0	20.0
blend	4640	4.0	12.0
HeII	4686	2.0	6.0
Hβ	4861	19.6	8.5
[OIII]	4959	10.0	8.0
[OIII]	5007	30.0	24.0
[FeVI]	5176	2.5	1.0
[CaV]	5309	1.0	1.2
[NII]	5755	5.7	7.5
HeI	5876	3.2	1.8
[FeVII]+[CaV]	6086	3.5	2.7
[FeX]	6375	1.3	1.6
Hα	6563	59.0	49.0
HeI	7065	2.4	3.0
[OII]	7320	1.6	3.4